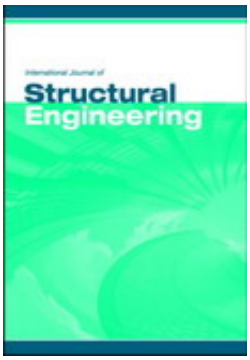

International Journal of Structural Engineering

ISSN online: 1758-7336 - ISSN print: 1758-7328
https://www.inderscience.com/ijstructe

A multilevel iterative algorithm for robust nonlinear dynamic analysis of force-based beam structure

Ausama Mohamed Ali, Jame Alexander, Tathagata Ray

DOI: 10.1504/IJSTRUCTE.2023.10060186

Article History:

Received:	18 November 2022
Last revised:	13 August 2023
Accepted:	15 August 2023
Published online:	26 February 2024

A multilevel iterative algorithm for robust nonlinear dynamic analysis of force-based beam structure

Ausama Mohamed Ali

Engineering and Industrial Technology,
North Shore Community College,
300 Broad Street, Lynn, MA 01905, USA
Email: amohamed@northshore.edu

Jame Alexander

H2B Inc.,
1225 N Loop W #800,
Houston, TX 77008, USA
Email: jame.alexander@outlook.com

Tathagata Ray*

Construction and Civil Engineering Technology,
Morehead State University,
105 A Llyod Cassity Building,
Morehead, KY 4035, USA
Email: t.ray@moreheadstate.edu
*Corresponding author

Abstract: Modelling material nonlinearity is imperative in structural analysis, especially for earthquake, blast, impact, and environment-driven chemical deteriorations. Stiffness-based beams are primarily used in commercial software for simulating such nonlinearity. This paper presents several improvements of the flexibility-based method to make it better than the stiffness-based method. The specific developments proposed here are: 1) the iterative convergence for updating the state of the element sections, and solution of the multi-axial smooth hysteretic equation; 2) the derivation of consistent tangent stiffness of the smooth hysteretic model; 3) the semi-implicit iteration for determining the incremental corotational stress resultants. The proposed solution is verified satisfactorily with existing stiffness-based solutions for global and local nonlinear dynamic responses. The proposed solution performs better than the existing stiffness-based solutions regarding coarser element discretisation and larger time-step. The chief reasons for this superior performance are: 1) the multilevel iterative algorithm; 2) the consistent tangent operator.

Keywords: nonlinear dynamic analysis; flexibility-based beam; stiffness-based beam; implicit solution algorithm.

Reference to this paper should be made as follows: Ali, A.M., Alexander, J. and Ray, T. (2024) 'A multilevel iterative algorithm for robust nonlinear dynamic analysis of force-based beam structure', *Int. J. Structural Engineering*, Vol. 14, No. 1, pp.25–41.

Biographical notes: Ausama Mohamed Ali is an Assistant Professor at Northshore Community College, MA, USA. He obtained his BS in Civil Engineering from the University of Anbar, Iraq. He obtained his MS in Civil Engineering from Dr. Babasaheb Ambedkar Marathwada University, India. He obtained his PhD in Civil Engineering from New Mexico State University. His research interests include structural analysis, structural dynamics, finite element analysis, earthquake engineering, finite element modelling, construction engineering, dynamic analysis, and nonlinear analysis.

Jame Alexander is a Professional Engineer and works at H2B Inc. He completed his undergraduate degree in Civil Engineering in 2006 at Carmel Engineering College under Mahatma Gandhi University, Kerala, India. He obtained his Master's in Structural Engineering in 2012 from Karunya University, Coimbatore, India. In his Master's thesis, he performed experimental work on investigating the effect of a scissor-jack damper system installed in a three-story steel moment-resisting frame under strong earthquakes. He obtained his PhD in Civil Engineering from New Mexico State University in 2019. His PhD dissertation was on seismic protection of structures through passive control.

Tathagata Ray received his BTech in Civil Engineering from the Indian Institute of Technology, Roorkee, and PhD in Structural and Earthquake Engineering from the State University of New York, University at Buffalo. He served as an Assistant Professor at New Mexico State University, as an Adjunct Faculty at the Oregon Institute of Technology, and as a Structural Design Engineer at PSE Consulting Engineers in Oregon. He joined Morehead State University as an Assistant Professor in Fall 2022. He teaches construction and civil engineering courses. His research interest includes designing buildings that can withstand extreme earthquakes and windstorms.

1 Introduction

Nonlinear response in structural and structural protective systems is observed in earthquake and wind-induced damage (Alexander et al., 2017; Ali et al., 2019; Belega et al., 2017; Bougteb and Ray, 2017; Ray, 2013, 2016; Ray and Reinhorn, 2012; Ray et al., 2013a, 2013b; Ray et al., 2015). It is observed in the blast and impact loadings (Anas and Alam, 2022; Anas et al., 2023a, 2023b, 2021a, 2021b, 2022). Environment driven chemical deterioration causes nonlinear response (Gong et al., 2023; Li et al., 2023; Sun et al., 2023; Wang et al., 2023). Functionally graded beams exhibit nonlinear behaviour (Ziou et al., 2016) as well. Hence, modelling nonlinear behaviour in a beam element for structural analysis is of paramount importance.

Material nonlinearity in a beam section is associated with the section's plasticisation and the extent of plasticisation throughout the member length. The displacement or stiffness-based formulation of beam elements invariably assumes that the plastic behaviour is concentrated at the end nodes of the beam. This assumption of concentrated plasticity is a 'mathematical abstraction because it implies infinite strains (Powell and Chen, 1986).' In force or flexibility-based beam formulation, it is ensured that the plasticity spreads along the member length, and the member sectional stress-resultants remain in equilibrium with the nodal stress-resultants. Plasticisation within the beam sections in force-based elements is modelled by two approaches. The first approach

discretises the section into several fibres or integration points. The hysteretic actions of stresses are monitored in these segments. Finally, the instantaneous segmental stiffness is integrated over the cross-section area to obtain the section stiffness matrix. This approach is also known as the fibre-based microscopic approach (Bäcklund, 1976; Belytschko and Hsieh, 1973; Carlson, 1999; Kunnath et al., 1990; Kunnath, 1988; Kyakula and Wilkinson, 2004; Park et al., 1987; Spacone et al., 1996a, 1996b; Zeris and Mahin, 1991). In the second approach, the global plasticisation of the section is monitored through the combined hysteretic actions of the sectional stress resultants. This method is called the section-level macroscopic approach (Kunnath and Reinhorn, 1990; Lee and Filippou, 2009; Powell and Chen, 1986; Ray, 2013; Reinhorn et al., 2009; Schachter and Reinhorn, 2010; Scott and Fenves, 2006; Scott et al., 2004; Sfakianakis and Fardis, 1991; Sivaselvan and Reinhorn, 2002). Other methods for modelling beam elements include the strut and tie method (Dashlejeh and Arabzadeh, 2019), first order elasto-plastic formulation, and the finite difference method (Rahman and Chowdhuri, 2010).

Despite the advantage regarding the spread of plasticity, it is to be noted that, barring a few (LARSA, 2016; Reinhorn et al., 2009), most commercial and academic structural analysis software (ABAQUS, 2016; ADINA, 2016; McKenna et al., 2016; SAP2000, 2016) use stiffness-based beam formulations for nonlinear dynamic analysis. The chief reason is that the stiffness-based formulation adheres to the general finite element analysis procedure, whereby the incremental global displacements are interpolated to obtain the incremental element strains. From the latter, the element states of stress-resultants and stiffness are updated. The force-based beam lacks the strain-displacement interpolation function. Further, the force-based beam requires iterations for section-level convergence, which is perceived to add up to the computational cost.

This paper proposes a novel procedure for nonlinear dynamic analysis of planar structures using the flexibility-corotational beam by performing the following convergence checks:

1 the iterative convergence check for updating the state of the element sections at GL nodes

2 the iterative convergence check for the solution of the multi-axial smooth hysteretic equation using the backward Euler formulation; in addition to the convergence check of global force vector at dynamic degrees of freedom.

Further, the consistent tangent stiffness for the smooth hysteretic model is derived, which enables faster convergence (Simo and Taylor, 1985). A semi-implicit procedure for predicting the direction vector of element corotational incremental stress-resultants is also proposed, which simulates the switching between the elastic and inelastic stiffness matrix of the beam section. These developments demonstrate that the force-based beam performs better than the stiffness-based beam's implementation in the state-of-the-art commercial software ABAQUS and ADINA, as far as:

a handling larger time steps

b coarser discretisation of the structure are concerned.

Section 2 describes the equilibrium of the beam element with both material and geometric nonlinearity. The state-of-the-art solution algorithm with state updating methods is described in Section 3. The proposed novel developments in the solution is described in Section 4. Verification of the proposed solution with existing stiffness-based

solutions from ABAQUS and ADINA is shown in Section 5. The advantages of the proposed solution algorithm over existing stiffness-based solutions are demonstrated in Section 6. Finally, the concluding remarks are given in Section 7.

2 Equilibrium statement of the geometrically nonlinear inelastic flexibility-corotational planar beam

In the corotational formulation by Ray (2016), Ray et al. (2015) (Figure 1), the rigid body movement of the element's chord with respect to a stationary global coordinate system (subscript *g*) and the member deformations (*qi*'s) in the corotational coordinate system (subscript *c*) are treated separately. The section orientation is expressed in the member coordinate system (subscript *m*).

The equation (2.1) represents the equilibrium of the beam section. $F^m \subset R^3$ is the stress-resultant vector (axial, shear, and moment) in the member coordinate, $F_o \subset R^3$ is the unidirectional yield value of F^m, and $\Delta\varepsilon^m \subset R^3$ is the work-conjugate (strains and curvatures) of F^m.

$$\begin{aligned} \Delta F^m &= \boldsymbol{k}^m \left(\Phi\left(F^m, F_o\right), \Delta F^m\right) \Delta\varepsilon^m \\ \boldsymbol{f}^m &= \left(\boldsymbol{k}^m\right)^{-1} \end{aligned} \tag{2.1}$$

$Q \subset R^3$ is the corotational stress resultant, whose work conjugates is the Δq (Figure 1). denotes the translational location of any beam section *j* with respect to the chord.

Figure 1 Coordinate systems, stress resultants (Qi), and displacements and rotations (*qi*) in corotational coordinates

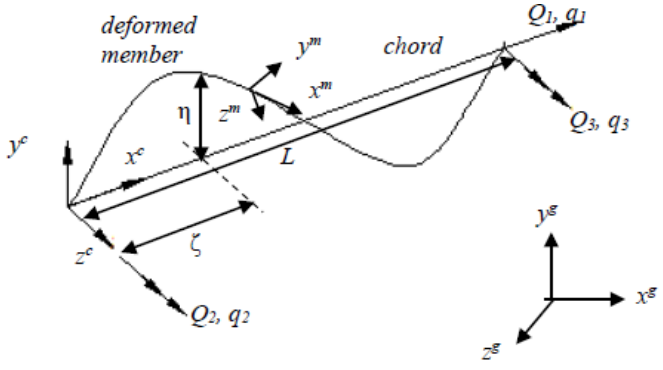

The Gauss-Lobatto (GL) integration points are chosen as it ensures that the end nodes of the beam, whose likelihood of attaining inelasticity is maximum, are included. $\Phi \subset R$ represents the multi-axial yield function of F^m. The continuum version of the smooth hysteretic model and the corresponding section stiffness matrix $\boldsymbol{k}^m$ (Ray et al., 2013) is expressed as follows.

$$\Delta F^m = (1-a)\boldsymbol{k_e}\left[\boldsymbol{I}\Delta\varepsilon^m - H_1H_2\partial\boldsymbol{\Phi}_{\boldsymbol{F}^{mh}}\boldsymbol{k_e}\Delta\varepsilon^m\left(\partial\boldsymbol{\Phi}_{\boldsymbol{F}^m}\right)^T \Big/ \left\{\partial\boldsymbol{\Phi}_{\boldsymbol{F}^{mh}}\boldsymbol{k_e}\left(\partial\boldsymbol{\Phi}_{\boldsymbol{F}^m}\right)^T\right\}\right] + a\boldsymbol{k_e}\Delta\varepsilon^m \tag{2.2}$$

$$H_1 = \left(\Phi\left(F^{mh}\right)\right)^N,\ H_2 = \left(1+sign\left(\left(F^{mh}\right)^T\left\{\Delta F^{mh}\right\}\right)\right)\Big/2,\ F^{mh} = (1-a)F^m$$

$$\boldsymbol{k^m} = (1-a)\boldsymbol{k_e}\left\{\boldsymbol{I} - H_1H_2\boldsymbol{I}\right\} + a\boldsymbol{k_e} \tag{2.3}$$

Here a is the post-elastic hardening coefficient. F^{mh} is the hysteretic part of the sectional stress resultants. $\boldsymbol{k_e}$ is the diagonal elastic stiffness matrix of the section involving the axial (AE), flexural (EI), and shear rigidities (GJ). N, H_1, and H_2 are scalar coefficients that control the smooth transition from the elastic to the inelastic stage. The consistent version of the section stiffness matrix will be derived later in this paper. The incremental equilibrium equation for the beam element in the corotational coordinate system is written as follows:

$$\Delta Q = \boldsymbol{k^c}\Delta q\left(\boldsymbol{k^c}\right)^{-1} = \boldsymbol{f^c} = \sum_{j=1}^{n}\left(\boldsymbol{B_j}^T\boldsymbol{f_j^m}w_jL/2\right) \tag{2.4}$$

$\boldsymbol{k_c}$ and $\boldsymbol{f^c}$ are the corotational stiffness and flexibility matrices, respectively. n is the total number of GL integration points (j) considered for integrating the section flexibility matrix $\boldsymbol{f_j^m}$ over the beam length (L), with weights w_j. $\boldsymbol{B}_j$ is the equilibrium matrix that maps Q onto F^m. It is expressed in terms of ζ_j, η_j, L, and the rotation matrix $\boldsymbol{R_j^m}$, per equation (2.5). θ_j^m denotes the section rotation with respect to the corotational coordinate at the j^{th} GL point.

$$F_j^m = \boldsymbol{B_j}Q$$
$$\boldsymbol{B_j} = \left(\boldsymbol{R_j^m}\right)^T\bar{\boldsymbol{B}}_{\boldsymbol{j}} \tag{2.5}$$
$$\bar{\boldsymbol{B}}_{\boldsymbol{j}} = \begin{bmatrix} 1 & 0 & 0 \\ 0 & -1/L & -1/L \\ \eta_j & \zeta_j/L-1 & \zeta_j/L \end{bmatrix},\qquad \boldsymbol{R_j^m} = \begin{bmatrix} \cos\left(\theta_j^m\right) & \sin\left(\theta_j^m\right) & 0 \\ -\sin\left(\theta_j^m\right) & \cos\left(\theta_j^m\right) & 0 \\ 0 & 0 & 1 \end{bmatrix}$$

The incremental equilibrium equation of the beam in global coordinates, which relates the global nodal stress resultant vector $F^g \subset R^6$ with its work conjugate $\Delta u^g \subset R^6$ is given by:

$$\Delta F^g = \Delta\boldsymbol{R}^{\boldsymbol{gl}T}\boldsymbol{Tr}^TQ + \boldsymbol{R}^{\boldsymbol{gl}T}\Delta\boldsymbol{Tr}^TQ + \boldsymbol{R}^{\boldsymbol{gl}T}\boldsymbol{Tr}^T\boldsymbol{k^c}\boldsymbol{TrR}^{\boldsymbol{gl}}\Delta u^g \tag{2.6}$$

$\boldsymbol{R}^{\boldsymbol{gl}}$ represents the chord's rotation matrix and is given similarly as $\boldsymbol{R_j^m}$ in the equation set (2.5). $\boldsymbol{Tr}$ maps Q onto the corotational coordinate's full (dependent) nodal stress resultant vectors. Equation (2.6) manifests a two-dimensional flexibility-corotational beam element's full geometric and material nonlinearity. By combining the individual terms on the right-hand side, the equation (2.6) can be expressed compactly as:

$$\Delta F^g = \boldsymbol{k^g}\Delta u^g \tag{2.7}$$

Here $\boldsymbol{k^g}$ is the instantaneous global stiffness matrix of the beam element. The performance of this element within the context of geometric nonlinearity is adequately demonstrated by Ray (2016). This paper will illustrate its capability to simulate material nonlinearity.

3 The solution of the nonlinear dynamic equation with state updating of the force-based beam element

The equation of motion of the structure for an input ground acceleration a_{gm} is expressed as:

$$\boldsymbol{m}\frac{d^2u}{dt^2}+\boldsymbol{c}\frac{du}{dt}+f_s=-\boldsymbol{m}a_{gm} \tag{3.1}$$

Here $\boldsymbol{m}$ is the dynamic mass matrix; $\boldsymbol{c}$ is the damping matrix. f_s is the nonlinear restoring force, and u is the displacement vector. The Newmark method with coefficients $\gamma = 0.5$, $\beta = 0.25$ is used. The element states, followed by the restoring force f_{si}, are updated per the following steps.

1 The global nodal incremental deformation vector Δu^g is obtained from Δu.

2 Δq is calculated as follows.

$$\Delta q = \boldsymbol{TrR^{gl}}\Delta u^g \tag{3.2}$$

3 ΔQ is obtained from Δq per section 4.

4 ΔF_j^m is obtained at each GL node from ΔQ by using the equation (2.5).

5 The vectors $\left(F_j^m, \varepsilon_j^m, \boldsymbol{k_j^m}\right)$ are updated per section 4. $\left(\zeta_j, \eta_j, \boldsymbol{R_j^m}\right)$ are updated per (Crisfield, 1997; Ray et al., 2015).

6 $\boldsymbol{R^{gl}}$ is updated using the quaternion-based process (Ray, 2016).

7 The updated Q is calculated as

$$Q = \frac{1}{n}\sum_{j=1}^{n}\left(\boldsymbol{B_j}\right)^{-1}F_j^m \tag{3.3}$$

8 The global convergence at dynamic degrees of freedom is checked as follows.

a The current dynamic restoring force f_{si} is obtained from F^g using the equation (3.4).

$$f_{si} \leftarrow F^g = \sum_{\#\,elements}\boldsymbol{R^{glT}Tr^T}Q \tag{3.4}$$

b The current unbalanced force Δf_{s_unbal} is calculated as follows.

$$\Delta f_{s\_unbal} = f_{so} + \Delta f_s - f_{si} \tag{3.5}$$

c Let the convergence tolerance be ε_f. The global convergence is checked as follows.

$$if\left(\left\|\Delta f_{s\_unbal}\right\|/\left\|f_{so}+\Delta f_s\right\|<\varepsilon_f\right)\Rightarrow converged \tag{3.6}$$

If the convergence check is failed, then the iteration restarted by solving the equation (3.1) and by setting $\Delta f_{s\_unbal}\rightarrow\Delta f_s$

9 Finally, u, $\dfrac{du}{dt},\dfrac{d^2u}{dt^2}$ are updated following standard procedures.

4 Proposed novel developments in the solution process

4.1 The proposed formulation of the consistent instantaneous stiffness of the smooth hysteretic model

Let us define Ψ as follows.

$$\Psi^T=\left(\partial\Phi_{\boldsymbol{F^{mh}}}\right)_{1x3} \tag{4.1}$$

The hysteretic part of the equation (2.2) gets modified as follows.

$$\begin{aligned}&F^{mh}-F_o^{mh}=f_1-f_2f_3\\&f_1=\boldsymbol{k_{eh}}\left(\varepsilon^m-\varepsilon_o^m\right),\quad f_2=H_2\Phi^N\boldsymbol{k_{eh}}\Psi/\left(\Psi^T\boldsymbol{k_{eh}}\Psi\right),\\&f_3=\left\{\Psi^T\boldsymbol{k_{eh}}\left(\varepsilon^m-\varepsilon_o^m\right)\right\},\ \boldsymbol{k_{eh}}=(1-a)\boldsymbol{k_e}\end{aligned} \tag{4.2}$$

F^{mh} and F_o^{mh} are the final and initial hysteretic section stress resultants. Similarly, the strains $\left(\varepsilon^m,\varepsilon_o^m\right)$ are defined. The *consistent* instantaneous stiffness is defined as follows.

$$\left(\partial F^{mh}/\partial\varepsilon^m\right)\Delta\varepsilon^m=\left(\partial_{\varepsilon^m}F^{mh}\right)\Delta\varepsilon^m=\boldsymbol{k_{cons}^m}\Delta\varepsilon^m \tag{4.3}$$

This can be found by taking the variation of the equation (4.2) as follows.

$$\left(\partial_{\varepsilon^m}F^{mh}\right)\Delta\varepsilon^m=\left(\partial_{\varepsilon^m}f_1\right)\Delta\varepsilon^m-f_3\left(\partial_{\varepsilon^m}f_2\right)\Delta\varepsilon^m-f_2\left(\partial_{\varepsilon^m}f_3\right)\Delta\varepsilon^m \tag{4.4}$$

The derivatives on the right-hand side of the equation (4.4) are given by equations (4.5)–(4.7).

$$\left(\partial_{\varepsilon^m}f_1\right)\Delta\varepsilon^m=\boldsymbol{k_{eh}}\Delta\varepsilon^m \tag{4.5}$$

$$\begin{aligned}\left(\partial_{\varepsilon^m}f_2\right)\Delta\varepsilon^m=&\Big[H_2\boldsymbol{k_{eh}}\Psi N\Phi^{N-1}\Psi^T\left(\partial_{\varepsilon^m}F^{mh}\right)\Delta\varepsilon^m+H_2\Phi^N\boldsymbol{k_{eh}}\left(\partial_{F^{mh}}\Psi\right)\\&\left(\partial_{\varepsilon^m}F^{mh}\right)\Delta\varepsilon^m\Big]/\left(\Psi^T\boldsymbol{k_{eh}}\Psi\right)\\&-H_2\Phi^N\boldsymbol{k_{eh}}\Psi\left\{2\Psi^T\boldsymbol{k_{eh}}^T\left(\partial_{F^{mh}}\Psi\right)\left(\partial_{\varepsilon^m}F^{mh}\right)\Delta\varepsilon^m\right\}/\left(\Psi^T\boldsymbol{k_{eh}}\Psi\right)^2\end{aligned} \tag{4.6}$$

$$\left(\partial_{\varepsilon^m}f_3\right)\Delta\varepsilon^m=\Psi^T\boldsymbol{k_{eh}}\Delta\varepsilon^m+\left(\varepsilon^m-\varepsilon_o^m\right)^T\boldsymbol{k_{eh}}^T\left(\partial_{F^{mh}}\Psi\right)\left(\partial_{\varepsilon^m}F^{mh}\right)\Delta\varepsilon^m \tag{4.7}$$

Using the equations (4.4) through (4.7), we get the following:

$$\begin{aligned}
&\boldsymbol{E_1}\left(\partial_{\varepsilon^m} F^{mh}\right)\Delta\varepsilon^m = E_2\Delta\varepsilon^m \\
&\boldsymbol{E_1} = \boldsymbol{I} + f_3\left\{\left\{H_2\boldsymbol{k_{eh}}\Psi N\Phi^{N-1}\Psi^T + H_2\Phi^N\boldsymbol{k_{eh}}\left(\partial_{F^{mh}}\Psi\right)\right\}\Big/\Psi^T\boldsymbol{k_{eh}}\Psi\right. \\
&\quad -\left\{2H_2\Phi^N\boldsymbol{k_{eh}}\Psi\Psi^T\boldsymbol{k_{eh}}^T\Psi^T\right\}\Big/\left(\Psi^T\boldsymbol{k_{eh}}\Psi\right)^2 \\
&\quad \left.+f_2\left\{\left(\varepsilon^m-\varepsilon_o^m\right)^T\boldsymbol{k_{eh}}^T\left(\partial_{F^{mh}}\Psi\right)\right\}\right\} \\
&\boldsymbol{E_2} = \boldsymbol{k_{eh}} - f_2\left\{\Psi^T\boldsymbol{k_{eh}}\right\}
\end{aligned} \tag{4.8}$$

Finally, considering the effect of the post elastic hardening, the consistent instantaneous stiffness is given by the equation (4.9).

$$\boldsymbol{k_{cons}^m} = \boldsymbol{E_1^{-1}E_2} + a\boldsymbol{k_e} \tag{4.9}$$

4.2 Proposed semi-implicit iteration for determining the incremental corotational stress resultant vector

After Δq is obtained from the equation (3.2), we must get ΔQ using $\boldsymbol{k^c}$. However, it can be realised that the formulation of $\boldsymbol{k^c}$ requires ΔF^m, which can only be determined if ΔQ is known. The following semi-implicit steps are proposed for this:

a Estimate ΔQ from the equation (2.4) using the existing $\boldsymbol{k^c}$.

b Estimate ΔF^m using the estimated ΔQ from the equation (2.5).

c Calculate the revised $\boldsymbol{k^c}$ using the estimated ΔF^m and the consistent tangent stiffness for the beam sections at GL nodes.

d Calculate the revised ΔQ from the equation (2.4).

4.3 Proposed implicit solution algorithm of the smooth hysteretic equation

For an incremental input strain $\Delta\varepsilon^m = \varepsilon - \varepsilon_o$ and the current stress resultant $(F^m)^0$, the equilibrated state of stress resultant F^m is calculated by solving the equation (2.2), which can be expressed through the backward Euler formalism as:

$$g := F^m - \left(F^m\right)^0 + h\left(F^m, \Delta\varepsilon^m\right) = 0 \tag{4.10}$$

Here $g,\ h \subset R^3$. Per the standard Newton-Raphson method of iteration, the updated iterative stress resultant state $(F^m)^{n+1}$ is given by the equation (4.11).

$$\left(F^m\right)^{n+1} = \left(F^m\right)^n - \left[\partial_{F^m} g\left(\left(F^m\right)^n, \Delta\varepsilon^m\right)\right]^{-1} g\left(\left(F^m\right)^n, \Delta\varepsilon^m\right) \tag{4.11}$$

Iterations are terminated when $\|g\|\Big/\left\|\left(F^m\right)^0 + h\left(F^m, \Delta\varepsilon^m\right)\right\| < \varepsilon_f$.

In the equation (4.11), $\partial_{F^m} g$ is calculated by assuming $\Delta\varepsilon$ as constant. Further, the derivatives are computed using the equations (4.5)–(4.7) with appropriate modifications.

The above method requires an initial guess for the stress state $(F^m)^0$. The nearer the guess to the final solution, the lesser the number of iterations. Hence $(F^m)^0$ is estimated here by using the last available consistent tangent stiffness as:

$$(F^m)^0 = (F^m)^0 + \boldsymbol{k}_{\boldsymbol{cons}}^{\boldsymbol{m}}\left((F^m)^0, \Delta\varepsilon^m\right)\Delta\varepsilon^m \tag{4.12}$$

Note that the above solution is performed for all the GL nodes in an element.

4.4 The proposed iterative process for element section state updating

Once ΔF_j^m 's are obtained from step 4 in section 3, F_j^m, ε_j^m, and $\left(\boldsymbol{k}_{\boldsymbol{cons}}^{\boldsymbol{m}}\right)_j$ are needed to be updated. The Newton-Raphson method is used for this update, as explained below.

a Calculate the trial $\Delta\varepsilon_j^m$ using the consistent tangent stiffness, as shown below.

$$\Delta\varepsilon_j^m = \left(\boldsymbol{k}_{\boldsymbol{cons}}^{\boldsymbol{m}}\right)_j^{-1}\Delta F_j^m \tag{4.13}$$

b Solve the equation (2.2) using $\Delta\varepsilon_j^m$ to generate the updated $F_{j\_updt}^m$.

c Check the convergence of the stress resultants as follows.

$$if \quad \left\|F_{j\_updt}^m - \left(F_j^m + \Delta F_j^m\right)\right\| \Big/ \left\|F_j^m + \Delta F_j^m\right\| < \varepsilon_f \rightarrow converged \tag{4.14}$$

d Update F_j^m, ε_j^m, and $\left(\boldsymbol{k}_{\boldsymbol{cons}}^{\boldsymbol{m}}\right)_j$.

e If convergence is not achieved, set and restart the iteration.

5 Verification of the proposed force-based beam structure simulation with the stiffness-based beam structure analysis

A two-bay two-story fixed base frame built with the AISC S20x66 beam, as shown in Figure 2, is modelled to verify the proposed developments. The steel yield strength is adopted as 344.74 MPa (= 50 ksi). The post-elastic hardening coefficient is adopted as 0.02 with kinematic hardening. The yield values of the axial (P_y), and bending moment (M_y) are adopted as 4,270.29 kN and 923.64 kN-m. The elastic modulus is adopted as 200 GPa. The horizontal translational mass lumped at each beam-column joint is 17,512.68 kN-sec^2/m (= 100 kips-s^2/inch). The mass density of the material is ignored. Modal damping of 5% is considered in all six dynamic modes. The convergence tolerance ε_f is assumed as 10^{-4}. The first 27 seconds of the 1,940 Imperial Valley accelerogram with input time steps of 0.02 sec and the peak acceleration scaled to 1.6 g is considered for the analysis. The acceleration is increased to subject the frame to severe nonlinearity so that the stability and robustness of the proposed solution can be tested.

The columns are assumed to carry zero initial axial loads. The following quadratic interaction between the axial load (P) and bending moment (M) is considered:

$$\Phi \equiv \left|P/P_y\right|^2 + \left|M/M_y\right|^2 - 1 = 0 \tag{5.1}$$

The stiffness-based analysis is simulated using the beam element of ABAQUS and ADINA (ABAQUS, 2016; ADINA, 2016) with fixed analysis time step dt = 0.00001 s. and four elements per member. The time step for the proposed force-based beam structure solution is adopted as dt = 0.0004 s, and one element with five GL nodes per

member is considered. Figure 3 compares the history of the story drifts between the proposed solution, ABAQUS, and ADINA. It can be observed that the responses from these solutions match appreciably. The maximum absolute difference in % story drift between the proposed and ABAQUS solutions is 2.5%, and that between the proposed and ADINA is 5%.

Figure 2 Elevation of the prototype frame

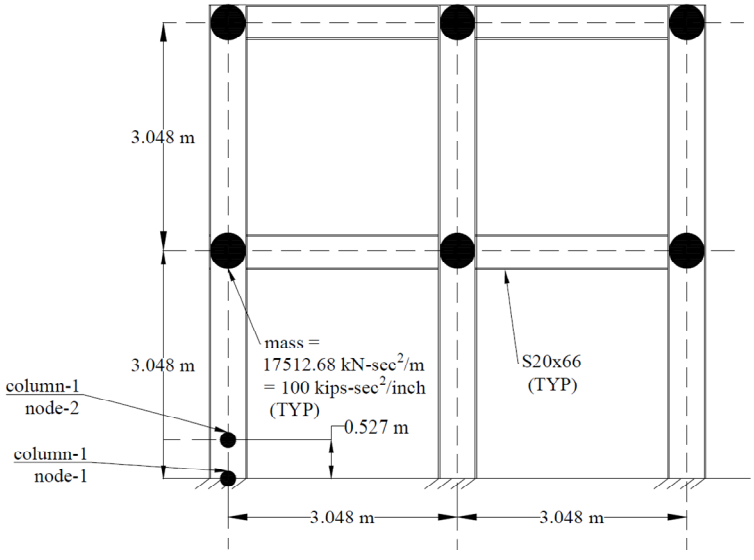

Figure 3 Comparison of the story drift responses between the proposed solution, ABAQUS, and ADINA

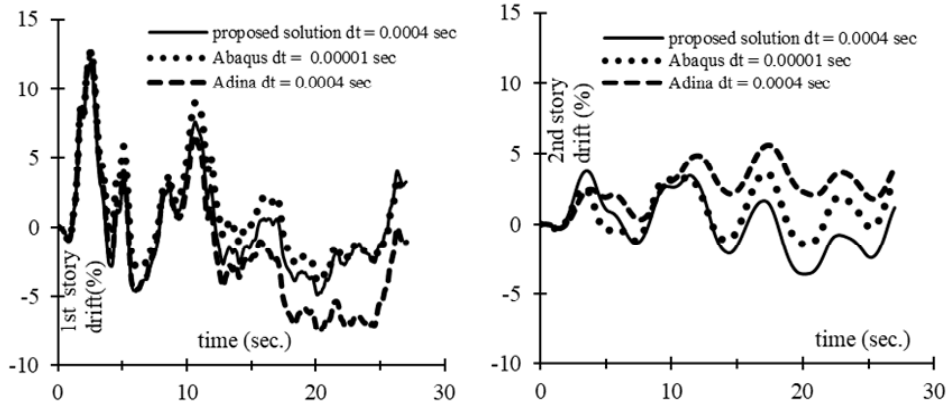

Figure 4 shows the comparison of the bending moment histories at the base node (node-1) and the GL node next to it (node-2) of column-1 (refer to Figure 2). The bending moment histories compare well, given that the ABAQUS and ADINA beam models are microscopic fibre-based and the proposed beam is macroscopic. The maximum absolute difference in the bending moment is 15%.

Figure 5 shows the moment-curvature (M-χ) responses from the proposed solutions for the two nodes mentioned above with two different time steps (dt = 0.02, 0.0004 s). It can be verified that the force-based beam can simulate the spread of plasticity along its length, as the M-χ response of node-2, which is adjacent to the base (refer to Figure 2), also shows hysteresis. The analysis with two different time steps shows some differences in curvatures. However, that difference does not spell much effect on the moment response and the global story drift response, as shown in section 6. In summary, it can be ascertained that the proposed solution with the macroscopic force-based beam compares well with the microscopic stiffness-based solutions.

Figure 4 Comparison of the bending moment responses between the proposed solution, ABAQUS, and ADINA (see online version for colours)

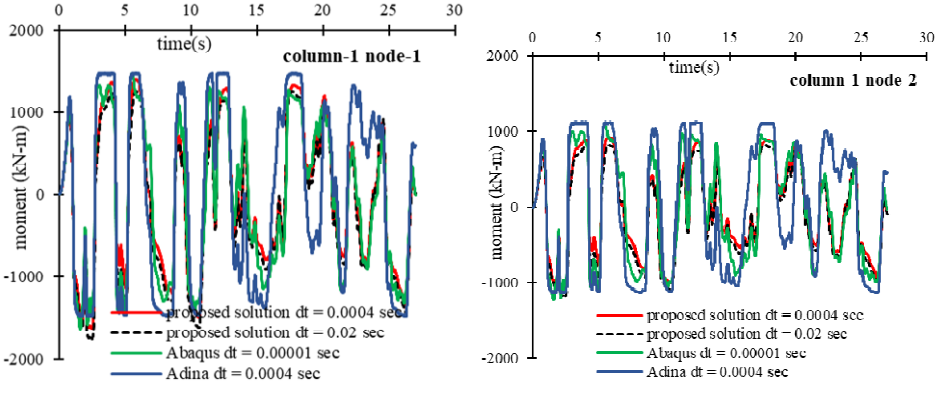

Figure 5 Moment-curvature hysteretic responses from the proposed solution for different time steps (see online version for colours)

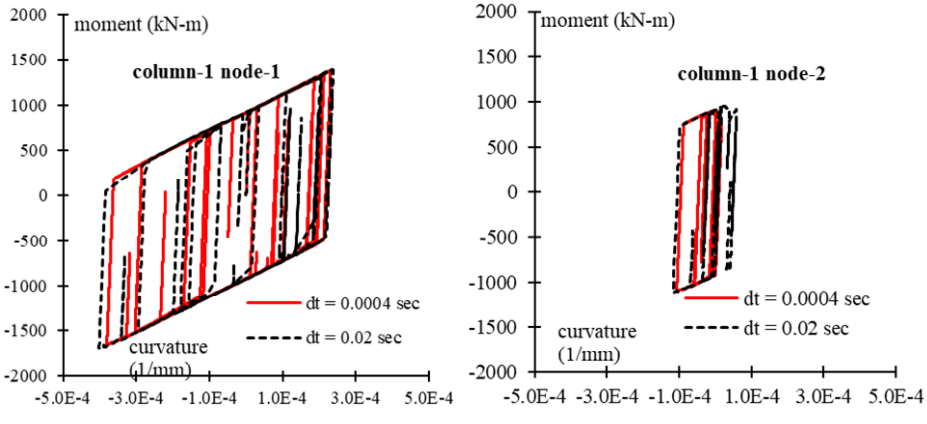

6 Advantages of the proposed force-based formulation over the stiffness-based formulation

6.1 The capability of handling larger time steps

The prototype structure with one element per member and 5 GL nodes per element is analysed with fixed time steps dt = 0.0004, 0.00667, 0.01, and 0.02 s (time step of the input ground motion). The story drift responses for all these cases are shown in Figure 6. The same structure with four elements per member was attempted to analyse in ABAQUS and ADINA with the same fixed time steps, with both full-Newton and quasi-Newton iterations. *However, the ABAQUS and ADINA solutions failed in all the cases with the error message that the fixed time increment was too large*. ABAQUS could produce a solution when variable dt = 0.02-0.00001s was allowed with automatic time increment. The same is true for ADINA with variable dt = 0.02-0.0004s. *Figure 6 shows that the proposed solution's responses are almost independent of the time steps, and the proposed solution can handle much larger time steps than the stiffness-based solutions of ABAQUS and ADINA.*

6.2 The capability of analysis with coarser discretisation

The prototype frame was analysed with the proposed force-based beam with one element per member but with 2, 3, 4, and 5 GL nodes per element. The analysis time step in each case was 0.02 sec. The story drift responses for all these cases are shown in Figure 7. With an increase in GL points, the solution converges. *Nevertheless, it is to be noted that the member discretisation was kept at one element per member, which is the coarsest possible. The maximum absolute difference in story drift between the 2-point and 5-point integration is less than 6%.*

Figure 6 Comparisons of the story drift responses from the proposed solutions with larger time steps

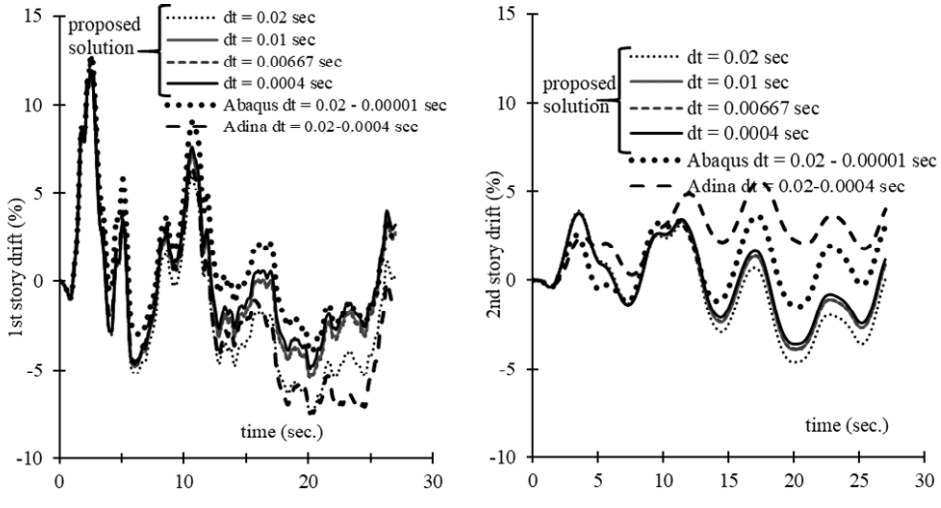

Figure 8 shows the story drift responses of the frame from the ABAQUS solution with 1, 2, 3, and 4 elements and dt = 0.02-0.00001 sec. It is observed that the responses converge with finer discretisation, as expected. However, the absolute difference between the responses with 1 and 4 element(s) per member is enormous (> 16%). Hence, it is ascertained that the proposed solution can handle coarser discretisation better than the implementation of the stiffness-based solution in ABAQUS. The similar solutions from ADINA (Figure 9) match quite well with each other. However, as noted earlier, ADINA solutions differed from ABAQUS and the proposed solutions when finer discretisation and smaller time steps were adopted.

As this formulation is tested for its robustness, sensitivity analyses with respect to coarser discretisation and larger time steps are done here. The study with various moduli of elasticity, post-elastic hardening, Py, My, etc. are appropriate for response spectrum analyses. Interested readers can find such a study in Sultana and Ray (2020).

Figure 7 Comparison of the story drift responses from the proposed solution with lesser gauss-LOBATTO (GL) points (see online version for colours)

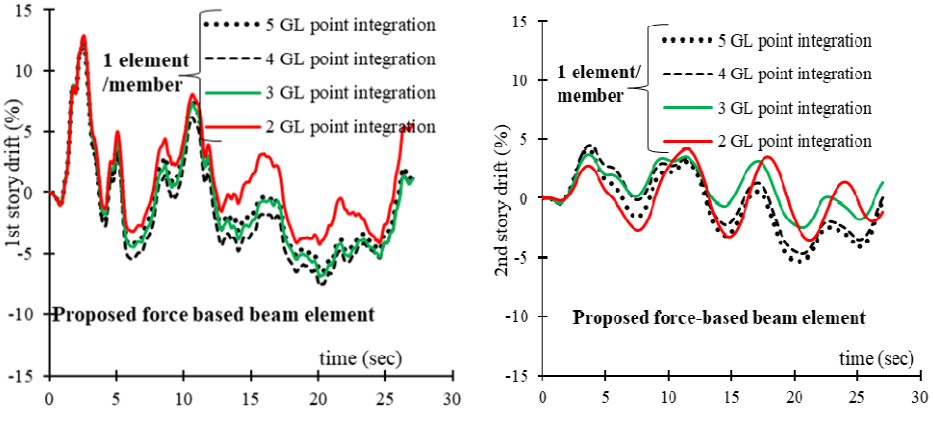

Figure 8 Comparison of the story drift responses from ABAQUS with coarser discretisation (see online version for colours)

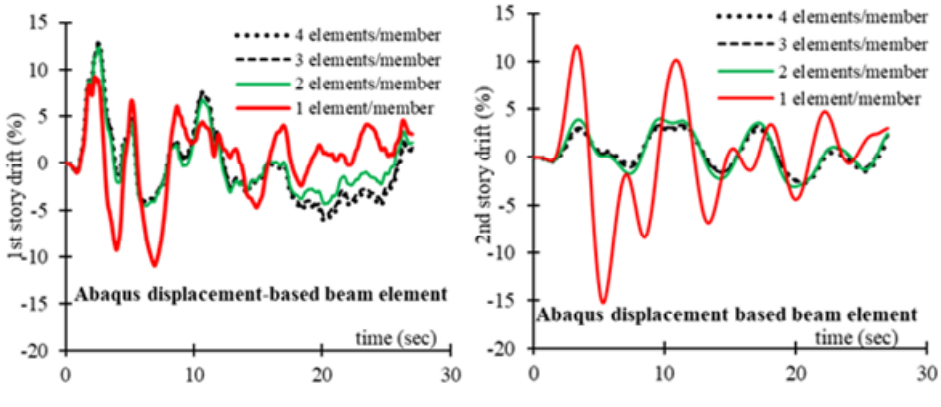

As this formulation is tested for its robustness, sensitivity analyses with respect to coarser discretisation and larger time steps are done here. The study with various moduli of elasticity, post-elastic hardening, Py, My, etc. are appropriate for response spectrum analyses. Interested readers can find such a study in Sultana and Ray (2020).

Figure 9 Comparison of the story drift responses from ADINA with coarser discretisation (see online version for colours)

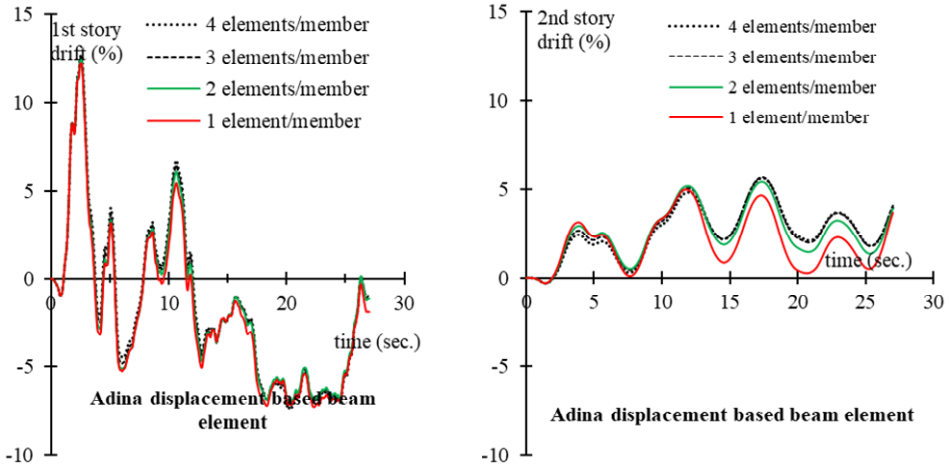

7 Concluding remarks

The paper discusses several developments in force-based beam structure's nonlinear dynamic solution process. These developments include:

1 updating the beam section's state of stress resultants, strain, and stiffness iteratively

2 a strain-driven solution of the smooth hysteretic equation using an iterative backward Euler formalism

3 a consistent tangent operator of the multi-axial smooth hysteretic model

4 prediction of the incremental corotational stress resultants by a semi-implicit integration.

The proposed solution is verified with state-of-the-art stiffness-based beam models from ABAQUS and ADINA. The two solutions' global story drift responses and the local beam sectional bending moment responses are compared well. The proposed solution also demonstrated the spread of plasticity along the beam length, as expected with the flexibility-based beam. It is further shown that the proposed solution performs better than the ABAQUS and ADINA solutions in handling larger time steps and coarser discretisation of the structure. The multilevel iterative process and consistent tangent operator used in the proposed formulation enabled these superior performances.

The application of this algorithm applies to both ductile and brittle materials. The multiaxial yield surface, as defined in the equation (2.1) and the post-elastic hardening coefficient a, as defined in the equations (2.2) and (2.3), will control ductility or

brittleness. The yield surface will shrink for brittle materials, and post-elastic hardening will be negative.

The current formulation for dynamic analysis is for two-dimensional beam elements. The authors will extend the same for three-dimensional beams with combined material and geometric nonlinearities.

References

ABAQUS (2016) *ABAQUS,* Dassault Systèmes Simulia Corp., Providence, RI, USA.

ADINA (2016) *Automatic Dynamic Incremental Nonlinear Analysis*, ADINA R & D, Inc., 71 Elton Avenue Watertown, MA 02472, USA.

Alexander, J. et al. (2017) 'Bicycle inspired adaptive self-centering device: development of the prototype, experimental results, and analytical predictions', *Journal of Structural Engineering*, Vol. 143, No. 9.

Ali, A.M. et al. (2019) 'Frequency-independent hysteretic dampers for mitigating wind-induced vibrations of tall buildings', *Structural Control and Health Monitoring*, Vol. 26, No. 5, p.e2341, https://onlinelibrary.wiley.com/doi/abs/10.1002/stc.2341.

Anas, S.M. and Alam, M. (2022) 'Comparison of existing empirical equations for blast peak positive overpressure from spherical free air and hemispherical surface bursts', *Iranian Journal of Science and Technology, Transactions of Civil Engineering*, Vol. 46, No. 2, pp.965–984, https://doi.org/10.1007/s40996-021-00718-4.

Anas, S.M. et al. (2021a) 'A study on existing masonry heritage building to explosive-induced blast loading and its response', International Journal of Structural Engineering, Vol. 11 No. 4, pp. 387-412 https://www.inderscienceonline.com/doi/abs/10.1504/IJSTRUCTE.2021.118065 (Accessed 2023/08/10 Access 2021).

Anas, S.M. et al. (2021b) 'Experimental and numerical investigations on performance of reinforced concrete slabs under explosive-induced air-blast loading: a state-of-the-art review', *Structures*, Vol. 31, pp.428–461 [online] https://www.sciencedirect.com/science/article/pii/S2352012421001090 (accessed 17 September 2023).

Anas, S.M. et al. (2022) 'Air-blast and ground shockwave parameters, shallow underground blasting, on the ground and buried shallow underground blast-resistant shelters: a review', *International Journal of Protective Structures*, Vol. 13, No. 1, pp.99–139, https://journals.sagepub.com/doi/abs/10.1177/20414196211048910.

Anas, S.M. et al. (202a3) 'Damage response of conventionally reinforced two-way spanning concrete slab under eccentric impacting drop weight loading', *Defence Technology*, Vol. 19, pp.12–34, https://www.sciencedirect.com/science/article/pii/S221491472200085X.

Anas, S.M. et al. (2023b) 'Influence of supports on the low-velocity impact response of square rc slab of standard concrete and ultra-high performance concrete: FEM-based computational analysis', *Buildings*, Vol. 13, No. 5, p.1220 [online] https://www.mdpi.com/2075-5309/13/5/1220.

Bäcklund, J. (1976) 'Large deflection analysis of elasto-plastic beams and frames', *Int. J. Mech. Sci*., Vol. 18, No. 6, pp.269–277.

Belega, B. et al. (2017) 'Effects of axial-shear-flexure interaction in static and dynamic responses of steel beams', *Journal of Constructional Steel Research*, Vol. 131, pp.83–93.

Belytschko, T. and Hsieh, B.J. (1973) 'Non-linear transient finite element analysis with convected coordinates', *Int. J. Numer. Methods Eng*., Vol. 7, pp.255–271.

Bougteb, Y. and Ray, T. (2017) 'Short communication: choice between series and parallel connection of hysteretic system and viscous damper for seismic protection of structures', *Earthquake Engineering and Structural Dynamics*, Vol. 47, No. 1, DOI: 10.1002/eqe.2938.

Carlson, A.E. (1999) *Three-Dimensional Nonlinear Inelastic Analysis of Steel Moment-Frame Buildings Damaged by Earthquake Excitations*, Report No. EERL 99-02.

Crisfield, M.A. (1997) *Nonlinear Finite Element Analysis of Solids and Structures*, John Wiley & Sons.

Dashlejeh, A.A. and Arabzadeh, A. (2019) 'Experimental and analytical study on reinforced concrete deep beams', *International Journal of Structural Engineering*, Vol. 10, No. 1, pp.1–24, https://www.inderscienceonline.com/doi/abs/10.1504/IJSTRUCTE.2019.101408 (accessed 8 October 2023).

Gong, F. et al. (2023) 'Computational modelling of combined frost damage and alkali–silica reaction on the durability and fatigue life of RC bridge decks', *Journal of Intelligent Construction*, Vol. 1, No. 1, p.9180001, https://doi.org/10.26599/JIC.2023.9180001.

Kunnath, S. et al. (1990) 'Analytical modeling of inelastic seismic response of r/c structures', journal of structural engineering, *A S C E*, Vol. 116, No. 4, pp.996–1017 http://ascelibrary.org/doi/abs/10.1061/%28ASCE%290733-9445%281990%29116%3A4%28996%29.

Kunnath, S.K. (1988) *Modeling of Inelastic Response and Seismic Damage of Three- Dimensional R/C Building Structures,* PhD, State University of New York, University at Buffalo.

Kunnath, S.K. and Reinhorn, A.M. (1990) 'Model for inelastic biaxial bending interaction of R/C beam-columns', *ACI Structural Journal*, Vol. 86, No. 3, pp.284–291.

Kyakula, M. and Wilkinson, S. (2004) 'An improved spread plasticity model for inelastic analysis of R/C frames subjected to seismic loading'. in *Conference An Improved Spread Plasticity Model for Inelastic Analysis of R/C Frames Subjected to Seismic Loading.*

LARSA (2016) *Larsa, Inc.*, 68 South Service Road, Suite 100, Melville, New York 11747.

Lee, C. and Filippou, F. (2009) 'Efficient beam-column element with variable inelastic end zones', *Journal of Structural Engineering*, Vol. 135, No. 11, pp.1310–1319 [online] http://ascelibrary.org/doi/abs/10.1061/%28ASCE%29ST.1943-541X.0000064.

Li, P. et al. (2023) 'A method to analyze the long-term durability performance of underground reinforced concrete culvert structures under coupled mechanical and environmental loads', *Journal of Intelligent Construction*, https://doi.org/10.26599/JIC.2023.9180011.

McKenna, F. et al. (2016) *The Open System for Earthquake Engineering Simulation*, Pacific Earthquake Engineering Research Center, University of California, Berkeley, CA, USA.

Park, Y.J. et al. (1987) *IDARC: Inelastic Damage Analysis of Reinforced Concrete Frame-Shear-Wall Structures*, Technical Report NCEER.

Powell, G. and Chen, P. (1986) '3D beam-column element with generalized plastic hinges', *Journal of Engineering Mechanics, A S C E*, Vol. 112, No. 7, pp.627–641 [online] http://ascelibrary.org/doi/abs/10.1061/%28ASCE%290733-9399%281986%29112%3A7%28627%29.

Rahman, M.A. and Chowdhuri, M.A.K. (2010) 'Experiment and non-linear analysis of stainless steel columns having variable cross-sections', *International Journal of Structural Engineering*, Vol. 1, Nos. 3–4, pp.312–326 [online] https://www.inderscienceonline.com/doi/abs/10.1504/IJStructE.2010.033485 (accessed 8 October 2023).

Ray, T. (2013) *Modeling of Multidimensional Nonlinear Elastic and Inelastic Structural Systems*, PhD, University at Buffalo, SUNY.

Ray, T. (2016) 'Enhanced solution scheme for nonlinear analysis of force-based beam for large rotations, multiple critical points, and random quasi-static loading input', *Journal of Structural Engineering*, Vol. 142, No. 9, http://ascelibrary.org/doi/abs/10.1061/%28ASCE%29ST.1943-541X.0001517.

Ray, T. and Reinhorn, A. (2012) 'Enhanced smooth hysteretic model with degrading properties', *Journal of Structural Engineering*, Vol. 140, No. 1, http://ascelibrary.org/doi/abs/10.1061/%28ASCE%29ST.1943-541X.0000798.

Ray, T. et al. (2013a) 'Hysteretic models for sliding bearings with varying frictional force', *Earthquake Engineering and Structural Dynamics*, Vol. 42, No. 15, pp.2341–2360, http://dx.doi.org/10.1002/eqe.2373.

Ray, T. et al. (2013b) 'Nonlinear elastic and inelastic spectra with inherent and supplemental damping', *Earthquake Engineering and Structural Dynamics*, Vol. 42, No. 14, pp.2151–2165, http://dx.doi.org/10.1002/eqe.2318.

Ray, T. et al. (2015) 'Flexibility-corotational formulation of space frames with large elastic deformations and buckling', *Computer-Aided Civil and Infrastructure Engineering*, Vol. 30, No. 1, pp.54–67, http://dx.doi.org/10.1111/mice.12084.

Reinhorn, A.M. et al. (2009) *IDARC2D Version 7.0: A Program for the Inelastic Damage Analysis of Structures*, Technical Report MCEER. (Access 2009)

SAP2000 (2016) *SAP2000 Integrated Finite Element Analysis and Design of Structures, Computers and Structures*, *Inc*., 1646 N. California Blvd., Suite 600 Walnut Creek, CA 94596 USA [online] http://books.google.com/books?id=ZpnwZwEACAAJ (accessed 17 September 2023).

Schachter, M. and Reinhorn, A.M. (2010) 'Dynamic analysis of three-dimensional frames with material and geometric nonlinearities', *Journal of Structural Engineering*, Vol. 137, No. 2, pp.207–219.

Scott, M. and Fenves, G. (2006) 'Plastic hinge integration methods for force-based beam–column elements', *Journal of Structural Engineering*, Vol. 132, No. 2, pp.244–252, http://ascelibrary.org/doi/abs/10.1061/%28ASCE%290733-9445%282006%29132%3A2%28244%29.

Scott, M.H. et al. (2004) 'Response sensitivity for nonlinear beam-column elements', *Journal of Structural Engineering*, Vol. 130, No. 9, pp.128–1288 [online] https://ascelibrary.org/doi/10.1061/%28ASCE%290733-9445%282004%29130%3A9%281281%29 (accessed 17 September 2023).

Sfakianakis, M. and Fardis, M. (1991) 'Bounding surface model for cyclic biaxial bending of RC sections', *Journal of Engineering Mechanics*, Vol. 117, No. 12, pp.2748–2769, http://ascelibrary.org/doi/abs/10.1061/%28ASCE%290733-9399%281991%29117%3A12%282748%29.

Simo, J.C. and Taylor, R.L. (1985) 'Consistent tangent operators for rate-independent elastoplasticity', *Computer Methods in Applied Mechanics and Engineering*, Vol. 48, No. 1, pp.101–118[online] http://www.sciencedirect.com/science/article/pii/0045782585900702.

Sivaselvan, M.V. and Reinhorn, A.M. (2002) 'Collapse analysis: large inelastic deformations analysis of planar frames', *Journal of Structural Engineering*, Vol. 128, No. 12, pp.1575–1583.

Spacone, E. et al. (1996a) 'Fibre beam-column model for non-linear analysis of R/C frames: Part 1. formulation', *Earthquake Engineering and Structural Dynamics*, Vol. 25, No. 7, pp.711–725, http://dx.doi.org/10.1002/(SICI)1096-9845(199607)25:7<711::AID-EQE576>3.0.CO;2-9.

Spacone, E. et al. (1996b) 'Mixed formulation of nonlinear beam finite element', *Computers and Structures,* Vol. 58, No. 1, pp.71–83 [online] https://www.sciencedirect.com/science/article/abs/pii/004579499500103N (accessed 17 September 2023).

Sultana, N. and Ray, T. (2020) 'Implications of bond-slip in inelastic dynamic responses of degrading structural systems', *International Journal of Civil Engineering*, Vol. 18, No. 9, pp.1039–1052, https://doi.org/10.1007/s40999-020-00522-7.

Sun, X. et al. (2023) 'Computational methods of mass transport in concrete under stress and crack conditions: a review', *Journal of Intelligent Construction*, https://doi.org/10.26599/JIC.2023.9180015.

Wang, Z. et al. (2023) 'Multi-scale and multi-chemo–physics lifecycle evaluation of structural concrete under environmental and mechanical impacts', *Journal of Intelligent Construction*, Vol. 1, No. 1, p.9180003, https://doi.org/10.26599/JIC.2023.9180003.

Zeris, C. and Mahin, S. (1991) 'Behavior of reinforced concrete structures subjected to biaxial excitation', *Journal of Structural Engineering*, Vol. 117, No. 9, pp.2657–2673, http://ascelibrary.org/doi/abs/10.1061/%28ASCE%290733-9445%281991%29117%3A9%282657%29.

Ziou, H. et al. (2016) 'Numerical modelling of a Timoshenko FGM beam using the finite element method', *International Journal of Structural Engineering*, Vol. 7, No. 3, pp.239–261 https://www.inderscienceonline.com/doi/abs/10.1504/IJSTRUCTE.2016.077719 (accessed 8 October 2023).